computation

MDPI

Article

Fractional-Order Degn–Harrison Reaction–Diffusion Model: Finite-Time Dynamics of Stability and Synchronization

Ma'mon Abu Hammad [1], Issam Bendib [2], Waseem Ghazi Alshanti [3], Ahmad Alshanty [4], Adel Ouannas [5], Amel Hioual [5,*] and Shaher Momani [6,7]

[1] Department of Mathematics, Al-Zaytoonah University of Jordan, Amman 11733, Jordan; m.abuhammad@zuj.edu.jo
[2] Applied Mathematics & Modeling Laboratory, Department of Mathematics, Faculty of Exact Sciences, University of Brothers Mentouri, Constantine 25000, Algeria; bendib.issam@doc.umc.edu.dz
[3] Department of Mathematics, Al Zaytoonah University of Jordan, Amman 11733, Jordan; w.alshanti@zuj.edu.jo
[4] Cyber Security Department, Al Zaytoonah University of Jordan, Amman 11733, Jordan; a.alshanty@zuj.edu.jo
[5] Department of Mathematics and Computer Science, University of Oum EL-Bouaghi, Oum El Bouaghi 04000, Algeria; ouannas.adel@univ-oeb.dz
[6] Nonlinear Dynamics Research Center (NDRC), Ajman University, Ajman 346, United Arab Emirates; s.momani@ajman.ac.ae
[7] Department of Mathematics, The University of Jordan, Amman 11942, Jordan
* Correspondence: amel.hioual@univ-oeb.dz

Abstract: This study aims to address the topic of finite-time synchronization within a specific subset of fractional-order Degn–Harrison reaction–diffusion systems. To achieve this goal, we begin with the introduction of a novel lemma specific for finite-time stability analysis. Diverging from existing criteria, this lemma represents a significant extension of prior findings, laying the groundwork for subsequent investigations. Building upon this foundation, we proceed to develop efficient dependent linear controllers designed to orchestrate finite-time synchronization. Leveraging the power of a Lyapunov function, we derive new, robust conditions that ensure the attainment of synchronization within a predefined time frame. This innovative approach not only enhances our understanding of finite-time synchronization, but also offers practical solutions for its realization in complex systems. To validate the efficacy and applicability of our proposed methodology, extensive numerical simulations are conducted. Through this comprehensive analysis, we aim to contribute valuable insights to the field of fractional-order reaction–diffusion systems while paving the way for practical implementations in real-world applications.

Keywords: finite-time synchronization; Degn–Harrison reaction–diffusion systems; finite-time stability; Lyapunov function

check for updates

Citation: Hammad, M.A.; Bendib, I.; Alshanti, W.G.; Alshanty, A.; Ouannas, A.; Hioual, A.; Momani, S. Fractional-Order Degn–Harrison Reaction–Diffusion Model: Finite-Time Dynamics of Stability and Synchronization. *Computation* **2023**, *12*, 144. https://doi.org/10.3390/computation12070144

Academic Editors: Endre Kovács, Denis Butusov and Valerii Ostrovskii

Received: 3 June 2024
Revised: 7 July 2024
Accepted: 10 July 2024
Published: 12 July 2024

Copyright: © 2023 by the authors. Licensee MDPI, Basel, Switzerland. This article is an open access article distributed under the terms and conditions of the Creative Commons Attribution (CC BY) license (https://creativecommons.org/licenses/by/4.0/).

1. Introduction

Developing appropriate controllers is essential for dynamic system analysis, particularly for achieving synchronization. Researchers have explored various mathematical models to understand the unique synchronization patterns of these systems. Mathematical models, such as reaction–diffusion equations, are employed to describe continuous-space systems like oscillating biological or chemical media, revealing complex dynamical structures such as bifurcations, spatial patterns, and turning instability. Studies suggest that reaction–diffusion systems, resembling low-dimensional oscillators, can exhibit synchronization. For instance, reference [1] examined synchronization in the Degn–Harrison reaction–diffusion system, reference [2] focused on synchronization control in the Lengyel–Epstein system, and reference [3] discussed synchronization in the FitzHugh–Nagumo model using a specific control approach. Over the past decade, there has been a significant increase in interest in fractional reaction–diffusion systems, especially regarding synchronization [4]. For example, in [5], synchronization in a specific type of fractional-order

spatiotemporal partial differential systems was investigated using the fractional Lyapunov technique. Furthermore, a hybrid approach was developed to synchronize between two integer and fractional-order reaction–diffusion systems, with applications to specific chemical models discussed in [6].

Within this framework, various methods and strategies have emerged to tackle the challenge of synchronizing partial differential equations. These approaches span a wide spectrum, encompassing active control techniques alongside both linear and nonlinear control schemes, as outlined in [7,8]. Diverse forms of synchronization have been delineated, each with its unique characteristics and applications. These include finite-time synchronization, phase synchronization, anticipated synchronization, complete synchronization, lag synchronization, function Q-S synchronization, projective synchronization, and generalized synchronization, as elaborated upon in references [9–11]. Through an extensive and thorough review of various methodologies, our objective is to delve deeply into the complexities of synchronization in partial differential equations. We aim to elucidate the diverse array of approaches that researchers and practitioners have developed and utilized within this field. By integrating insights from a broad spectrum of existing literature and synthesizing the collective findings of numerous past studies, we aspire to make a meaningful contribution to the ongoing scholarly conversation surrounding synchronization theory. Our work not only highlights the current state of research, but also identifies potential pathways for future advancements, thereby fostering further progress in this critical area of study.

Finite-time synchronization refers to a particular type of synchronization where coordinated behavior among systems is attained within a predetermined and finite time interval. Unlike traditional synchronization, which might require an indefinite period to converge, finite-time synchronization ensures that systems achieve synchrony within a defined time frame. This concept finds applications across various fields, such as control systems, communication networks, and robotics. For example, in the field of robotics, finite-time synchronization can enhance the efficiency and collaboration among multiple robotic agents by guaranteeing their coordinated movement within a designated time period. In communication networks, rapid synchronization is crucial for ensuring effective and reliable data transmission, as highlighted in references [12–15]. Despite its importance, research on finite-time synchronization of spatially extended systems described by reaction–diffusion systems (RDSs) remains limited.

In recent years, various numerical methods have been developed to solve reaction–diffusion equations effectively. Standard methods such as finite difference, finite element, and spectral methods have been widely used due to their robustness and computational efficiency [16–18]. Advancements in numerical analysis have led to more techniques, such as adaptive mesh refinement and parallel computing, enhancing the accuracy and efficiency of simulations. For fractional-order systems like the Degn–Harrison reaction–diffusion model, specialized methods such as fractional finite difference and fractional spectral methods have been proposed. These methods effectively address the unique challenges of fractional derivatives and provide deeper insights into the system's dynamics [19,20].

This research presents a significant and original contribution to the study of finite-time synchronization within a particular subset of fractional-order spatiotemporal partial differential systems. Our main goal is to conduct a comprehensive examination of both finite-time stability and finite-time synchronization in interconnected fractional reaction–diffusion systems. These systems are characterized by their complex dynamic behaviors, which are influenced by spatial and temporal variables, making them challenging yet crucial to study. To achieve finite-time stability, we employ a fractional Lyapunov method. This approach involves constructing a suitable Lyapunov function that helps in deriving the conditions under which the system's equilibrium point can be reached in a finite amount of time. This method is pivotal, as it ensures that the system's state will converge to the desired equilibrium within a predetermined timeframe, thereby enhancing the predictability and control of such systems. For attaining finite-time synchronization, we suggest a robust linear

control technique. This control strategy is designed to synchronize the states of fractional reaction–diffusion systems, ensuring that they exhibit coordinated behavior within a finite time interval. Our approach is general enough to be applicable to a wide range of fractional reaction–diffusion systems, making it a versatile tool for researchers and practitioners in the field. To illustrate the efficacy and practicality of our proposed control methods, we conduct detailed analyses of the synchronization behaviors of interconnected fractional-order Degn–Harrison systems. These systems serve as a representative example due to their complexity and relevance in various applications. Through simulations and theoretical analysis, we demonstrate how our control techniques can effectively achieve finite-time synchronization, thereby validating the robustness and applicability of our approach.

The paper is structured as follows: In Section 2, we delve into the foundational principles of fractional calculus, providing readers with a comprehensive understanding of the mathematical underpinnings essential for grasping the subsequent discussions. Section 3 provides a description of the Degn-Harrison models. Section 4 aims to investigate the finite-time stability of equilibrium points in reaction-diffusion models. This analysis is crucial for understanding the transient behavior of the system and determining whether it can achieve a stable state within a finite time. The practical implications of this analysis are significant, including applications in control system design, pattern formation in chemical and biological processes, and the synchronization of dynamic systems. Section 5 focuses on establishing a finite-time synchronization scheme for reaction-diffusion systems, specifically through the study of the Degn-Harrison reaction-diffusion system. Section 6 presents a diverse set of examples to illustrate the principles of finite-time stability and finite-time synchronization within the Degn-Harrison system.

2. Basic Tools

The aim of this section is to introduce the fundamental definitions and key theorems associated with fractional calculus, which are essential for understanding the subsequent analysis.

Definition 1 ([21,22]). *The Riemann–Liouville fractional-order integral operator of an arbitrary integrable function $\mathcal{E}$ can be defined as:*

$$\mathcal{I}_{\mathfrak{z}}^{\aleph}\mathcal{E}(\mathfrak{z}) = \frac{1}{\Gamma(\aleph)}\int_0^{\mathfrak{z}}(\mathfrak{z}-\varsigma)^{\aleph-1}\mathcal{E}(\varsigma)d\varsigma, \tag{1}$$

where $\mathfrak{z} \geq 0, 0 < \aleph < 1$, and $\Gamma(.)$ is the gamma function.

Definition 2 ([21,22]). *The Caputo fractional derivative of $\mathcal{E}$ is defined as:*

$${}_0^{C}\mathcal{D}_{\mathfrak{z}}^{\aleph}\mathcal{E}(\mathfrak{z}) = \frac{1}{\Gamma(1-\aleph)}\int_0^{\mathfrak{z}}(\mathfrak{z}-\varsigma)^{-\aleph}\frac{d}{d\varsigma}\mathcal{E}(\varsigma)d\varsigma, \tag{2}$$

where $0 < \aleph < 1$.

We consider the following fractional-order nonlinear system:

$$\begin{cases} {}_0^{C}\mathcal{D}_{\mathfrak{z}}^{\aleph}\mathcal{E}(\mathfrak{z}) = \chi(\mathfrak{z},\mathcal{E}(\mathfrak{z})), \quad \aleph \in (0,1), \mathfrak{z} > 0, \\ \mathcal{E}(0) = \mathcal{E}_0. \end{cases} \tag{3}$$

where $\chi : \mathbb{R}^n \to \mathbb{R}^n, \mathcal{E}(\mathfrak{z}) \in \mathbb{R}^n$, and ${}_0^{C}\mathcal{D}_{\mathfrak{z}}^{\aleph}$ is the Caputo fractional derivative of order $\aleph$, and a point $\mathcal{E}^* \in \mathbb{R}^n$ is an equilibrium point of fractional-order nonlinear system (3) if $\chi(\mathcal{E}^*) \equiv 0$.

Definition 3 ([23]). *$\mathcal{E}^*$ is called as the initial equilibruim point of fractional-order nonlinear system (3) if $\mathcal{E}_0 = \mathcal{E}^*$, or equivalently, $\mathcal{E}(\mathfrak{z}) \equiv \mathcal{E}^*, \forall \mathfrak{z} \in [\mathfrak{z}^*, +\infty)$.*

Definition 4 ([23]). *$\mathcal{E}^*$ is called as the finite-time equilibrium point of fractional-order nonlinear system (3) if there is a $\mathfrak{z}^* > 0$, such that $\mathcal{E}(\mathfrak{z}) \neq \mathcal{E}^*, \mathfrak{z} \in [0, \mathfrak{z}^*)$, and $\mathcal{E}(\mathfrak{z}) \equiv \mathcal{E}^*, \forall \mathfrak{z} \in [\mathfrak{z}^*, +\infty)$.*

Definition 5 ([23]). *Suppose $D \subseteq \Omega$ is an open neighborhood of 0, if there is a function $\mathfrak{z}^*(\mathcal{E}_0) : D\backslash\{0\} \to \mathbb{R}^*_+$ called the setting-time satisfying the upcoming conditions, then $\mathcal{E}^*$ is called a finite-time stable equilibrium point of the system (3).*

1. *$\forall \mathcal{E}_0 \in D\backslash\{0\}, \mathcal{E}(\mathfrak{z}) = \mathcal{E}(\mathfrak{z}, \mathcal{E}_0) \in D\backslash\{0\}, \forall \mathfrak{z} \in [0, \mathfrak{z}^*(\mathcal{E}_0)), \lim_{\mathfrak{z} \to \mathfrak{z}^*(\mathcal{E}_0)} \mathcal{E}(\mathfrak{z}) = 0$, and $\mathcal{E}(\mathfrak{z}) \equiv 0$ for $\mathfrak{z} \in [\mathfrak{z}^*(\mathcal{E}_0), +\infty)$.*
2. *For every open neighborhood U_ϵ of 0, there is an open subset U_δ containing 0 in D, such that for $\forall \mathcal{E}_0 \in U_\delta\backslash\{0\}$ and $\forall \mathfrak{z} \in [0, \mathfrak{z}^*(\mathcal{E}_0)), \mathcal{E}(\mathfrak{z}) = \mathcal{E}(\mathfrak{z}, \mathcal{E}_0) \in U_\varepsilon$.*

Theorem 1 ([23]). *$\mathcal{E}^*$ is an finite-time stability equilibrium point of the fractional-order nonlinear systems (3) if there exists a differentiable Lyapunov function $\mathcal{L} : [0, +\infty) \times \Omega \to \mathbb{R}_+$. three class $\mathcal{M}$ functions $\beta_1, \beta_2, \beta_3$, and $\delta > 0$ such that*

1. *$\beta_1 \|\mathcal{E}(\mathfrak{z})\| \leq \mathcal{L}(\mathfrak{z}, \mathcal{E}(\mathfrak{z})) \leq \beta_2 \|\mathcal{E}(\mathfrak{z})\|$,*
2. *$\mathcal{L}'(\mathfrak{z}, \mathcal{E}(\mathfrak{z})) < -\beta_3 \mathcal{E}(\mathfrak{z}, \mathcal{E}(\mathfrak{z}))$,*
3. *$\int_0^\epsilon \frac{d\mathcal{E}}{\beta_3(\mathcal{E})} < +\infty, (\forall \epsilon : 0 < \epsilon \leq \delta)$.*

Lemma 1 ([24,25]). *For all $\mathcal{E}(\mathfrak{z}) \in \mathbb{R}^n$ and $\aleph \in (0, 1)$, the following inequality holds*

$$ {}_0^C\mathcal{D}_\mathfrak{z}^\aleph \left(\mathcal{E}^\mathrm{T}(\mathfrak{z})\mathcal{E}(\mathfrak{z})\right) \leq 2\mathcal{E}^\mathrm{T}(\mathfrak{z}) {}_0^C\mathcal{D}_\mathfrak{z}^\aleph \mathcal{E}(\mathfrak{z}), \quad \mathfrak{z} \geq 0. \tag{4} $$

Definition 6 ([26]). *The Mittag–Leffler function with $\aleph > 0$ noted by $\mathsf{E}_\aleph$ and defined by*

$$ \mathsf{E}_\aleph(\mathfrak{z}) = \sum_{\mathrm{j}=0}^{+\infty} \frac{\mathfrak{z}^\aleph}{\Gamma(\aleph \mathrm{j} + 1)}, \tag{5} $$

Theorem 2 ([27]). *Let $\mathcal{L}(\mathfrak{z})$ be a continuous and positive definite function which satisfies*

$$ {}_0^C\mathcal{D}_\mathfrak{z}^\aleph \mathcal{L}(\mathfrak{z}) \leq -\mathfrak{Q}\mathcal{L}(\mathfrak{z}), \quad \forall \mathfrak{z} \geq 0, \tag{6} $$

where $0 < \aleph < 1$ and $\mathfrak{Q}$ is a positive constant. Then,

$$ \mathcal{L}(\mathfrak{z}) \leq \mathcal{L}(0)\mathsf{E}_\aleph\left(-\mathfrak{Q}\mathfrak{z}^\aleph\right), \quad \forall \mathfrak{z} \in [0, \mathfrak{z}^*), \tag{7} $$

where $\mathsf{E}_\aleph$ is a Mittag–Leffler function, with the setting time.

$$ \mathfrak{z}^* = \left(\frac{\Gamma(\aleph + 1)}{\mathfrak{Q}}\right)^{\aleph^{-1}}, \tag{8} $$

Moreover, $\mathcal{L}(0)$ is positive and $\mathcal{L}(\mathfrak{z}) = 0$ for $\mathfrak{z} \geq \mathfrak{z}^*$.

3. Description of the Models

The Degn–Harrison system illustrates the reaction process involving two substances: oxygen, denoted as $\mathcal{E}_1$, and a nutrient, denoted as $\mathcal{E}_2$. A key aspect of this system is that an excess of oxygen inhibits respiration, which is represented by a nonlinear rate function $\frac{\mathcal{E}_1}{1 + \mathfrak{q}\mathcal{E}_1^2}$. This function captures the saturation effect, where the inhibitory influence of oxygen increases with its concentration, but levels off due to the presence of the quadratic term in the denominator.

Considering that similar inhibitory phenomena can be described using comparable reaction schemes, we extend the inhibitory law using the same nonlinear function $\frac{\mathcal{E}_1}{1 + \mathfrak{q}\mathcal{E}_1^2}$.

This extension allows for the modeling of a broader range of reaction processes where inhibition plays a crucial role.

The reaction–diffusion model established based on this extended inhibitory law is known as the Degn–Harrison reaction–diffusion model. This model is characterized by partial differential equations that describe the spatial and temporal evolution of the concentrations of $\mathcal{E}_1$, and $\mathcal{E}_2$, The governing equations for the Degn–Harrison reaction–diffusion model are given by:

$$\begin{cases} {}_0^C\mathcal{D}_\mathfrak{z}^\aleph \mathcal{E}_1(\mathfrak{r},\mathfrak{z}) = \mathfrak{k}_1 \Delta \mathcal{E}_1 + \mathfrak{a} - \mathcal{E}_1 - \frac{\mathcal{E}_1 \mathcal{E}_2}{1+\mathfrak{q}\mathcal{E}_1^2}, & \mathfrak{r} \in \Omega, \mathfrak{z} > 0, \\ {}_0^C\mathcal{D}_\mathfrak{z}^\aleph \mathcal{E}_2(\mathfrak{r},\mathfrak{z}) = \mathfrak{k}_2 \Delta \mathcal{E}_2 + \mathfrak{b} - \frac{\mathcal{E}_1 \mathcal{E}_2}{1+\mathfrak{q}\mathcal{E}_1^2}, & \mathfrak{r} \in \Omega, \mathfrak{z} > 0, \\ \dfrac{\partial \mathcal{E}_1}{\partial \mathfrak{r}} = \dfrac{\partial \mathcal{E}_2}{\partial \mathfrak{r}} = 0, & \mathfrak{r} \in \partial\Omega, \mathfrak{z} > 0, \\ \mathcal{E}_1(\mathfrak{r},0) = \mathcal{E}_{1,0}(\mathfrak{r}) > 0, \quad \mathcal{E}_2(\mathfrak{r},0) = \mathcal{E}_{2,0}(\mathfrak{r}) > 0, & \mathfrak{r} \in \Omega. \end{cases} \tag{9}$$

In this context, Ω represents a bounded domain in $\mathbb{R}^n$ with a sufficiently smooth boundary, denoted as $\partial\Omega$. The coefficients $\mathfrak{k}_1$ and $\mathfrak{k}_2$ indicate the diffusion rates of the reactants $\mathcal{E}_1$ and $\mathcal{E}_2$, respectively. The parameter $\mathfrak{q}$ acts as a scaling factor influencing the strength of interaction between the variables $\mathcal{E}_1$ and $\mathcal{E}_2$. These diffusion coefficients are crucial parameters that determine how quickly substances spread throughout the domain Ω.

The constants $\mathfrak{a}$, $\mathfrak{b}$, $\mathfrak{q}$, $\mathfrak{k}_1$, and $\mathfrak{k}_2$ are assumed to be positive throughout the reaction process. These constants typically represent reaction rate parameters and other specific characteristics of the system's kinetics.

The Laplace operator, which accounts for the spatial diffusion of the reactants, is denoted by Δ. In an n-dimensional space, the Laplace operator is defined as:

$$\Delta = \sum_{i=1}^{n} \frac{\partial^2}{\partial \mathfrak{r}_i^2},$$

where $\frac{\partial^2}{\partial \mathfrak{r}_i^2}$ represents the second partial derivative with respect to the i-th spatial coordinate $\mathfrak{r}_i$. References [28,29] provide further mathematical background and applications of the Laplace operator in reaction–diffusion systems, emphasizing its importance in describing the spatial aspects of the process.

The reaction–diffusion model, incorporating these definitions and assumptions, is crucial for analyzing the behavior of the Degn–Harrison system under the influence of diffusion and nonlinear reactions. The precise formulation of the model allows for a detailed study of the dynamics and synchronization properties of the system within the domain Ω.

4. Stability Analysis

The aim of investigating finite-time stability equilibrium points in reaction–diffusion models is to understand the transient behavior of the system and determine whether it can settle into a stable state within a finite time frame. This type of analysis is crucial for predicting the system's behavior over limited time periods, which has significant implications for various practical applications. These applications include the design of control systems, the formation of patterns in chemical and biological processes, and the synchronization of dynamic systems.

In our study, we focus on a unique equilibrium point, which serves as the solution to the following system of Equation (10). By analyzing this equilibrium point, we can gain insights into the stability and synchronization properties of the reaction–diffusion

system. This analysis helps in ensuring that the system reaches a desired state quickly and maintains that state despite the presence of disturbances or variations in initial conditions.

$$\begin{cases} \mathfrak{k}_1 \Delta \mathcal{E}_1^* + \mathfrak{a} - \mathcal{E}_1^* - \frac{\mathcal{E}_1^* \mathcal{E}_2^*}{1+\mathfrak{q}\mathcal{E}_1^{*2}} = 0, \\ \mathfrak{k}_2 \Delta \mathcal{E}_2^* + \mathfrak{b} - \frac{\mathcal{E}_1^* \mathcal{E}_2^*}{1+\mathfrak{q}\mathcal{E}_1^{*2}} = 0, \end{cases} \tag{10}$$

The unique equilibrium point of systems (10) is given by

$$\mathcal{E}^* = (\mathcal{E}_1^*, \mathcal{E}_2^*) = \left(\mathfrak{a} - \mathfrak{b}, \mathfrak{b} \frac{1 + \mathfrak{q}(\mathfrak{a} - \mathfrak{b})^2}{\mathfrak{a} - \mathfrak{b}} \right), \tag{11}$$

Lemma 2 ([30]). *The following inequality holds*

$$\left| \frac{\bar{\mathcal{E}}_1 \bar{\mathcal{E}}_2}{1 + \mathfrak{q}\bar{\mathcal{E}}_1^2} - \frac{\mathcal{E}_1 \mathcal{E}_2}{1 + \mathfrak{q}\mathcal{E}_1^2} \right| \leq \mathfrak{P}(|\bar{\mathcal{E}}_1 - \mathcal{E}_1| + |\bar{\mathcal{E}}_2 - \mathcal{E}_2|), \tag{12}$$

where

$$\mathfrak{P} \geq \max\left\{ \frac{5}{4}\mathfrak{K}, \frac{1}{2\sqrt{\mathfrak{q}}} \right\}, \quad |\overline{\mathcal{E}_2}| < \mathfrak{K}. \tag{13}$$

Lemma 3 ([31]). *Ω is a bounded region in $\mathbb{R}^m$ with a smooth boundary denoted by $\partial\Omega$, which belongs to class $\mathcal{C}^2$. $\Xi(\mathfrak{r}) \in H_0^1(\Omega)$ represents a real-valued function, and $\frac{\partial \Xi(\mathfrak{r})}{\partial \eta}|_{\partial\Omega} = 0$. Then,*

$$\zeta_1 \int_\Omega |\Xi(\mathfrak{r})|^2 d\mathfrak{r} \leq \int_\Omega |\nabla \Xi(\mathfrak{r})|^2 d\mathfrak{r}, \tag{14}$$

where ζ_1 is determined as the positive eigenvalue of the following problem:

$$\begin{cases} -\Delta \Xi(\mathfrak{r}) = \zeta \Xi(\mathfrak{r}), & \mathfrak{r} \in \Omega, \\ \frac{\partial \Xi(\mathfrak{r})}{\partial \eta} = 0, & \mathfrak{r} \in \partial\Omega. \end{cases} \tag{15}$$

Theorem 3. *The equilibrium point $\mathcal{E}^* = \left(\mathfrak{a} - \mathfrak{b}, \mathfrak{b} \frac{1 + \mathfrak{q}(\mathfrak{a} - \mathfrak{b})^2}{\mathfrak{a} - \mathfrak{b}} \right)$ represents a finite-time stable equilibrium point of the fractional-order nonlinear systems (9), provided that he following conditions are satisfied:*

$$|\mathcal{E}_2| < \mathfrak{K}, \quad \mathfrak{P} \geq \max\left\{ \frac{5}{4}\mathfrak{K}, \frac{1}{2\sqrt{\mathfrak{q}}} \right\}, \quad \min\{\mathfrak{k}_1\zeta_1 - 2\mathfrak{P} + 1, \mathfrak{k}_2\zeta_2 - 2\mathfrak{P}\} > 0. \tag{16}$$

The time of finite-time stability of equilibrium point is estimated as

$$\mathfrak{z}_1^* = \frac{\mathcal{L}_2(0)}{2\min\{\mathfrak{k}_1\zeta_1 - 2\mathfrak{P} + 1, \mathfrak{k}_2\zeta_2 - 2\mathfrak{P}\}\mathcal{L}_2(\mathfrak{z}_{\max})}. \tag{17}$$

Proof. We construct the positive Lyapunov function as follows:

$$\mathcal{L}_2(\mathfrak{z}) = \frac{1}{2} \int_\Omega (\mathcal{E}_1 - \mathcal{E}_1^*)^2 + (\mathcal{E}_2 - \mathcal{E}_2^*)^2 \, d\mathfrak{r}, \tag{18}$$

where ${}_0\mathcal{D}_\mathfrak{z}$ denotes the normal derivative. According to Lemma 2, thus, we obtain:

$$
\begin{aligned}
{}_0\mathcal{D}_{\mathfrak{z}}\mathcal{L}_2(\mathfrak{z}) &= \frac{1}{2}\int_\Omega {}_0\mathcal{D}_{\mathfrak{z}}(\mathcal{E}_1-\mathcal{E}_1^*)^2+{}_0\mathcal{D}_{\mathfrak{z}}(\mathcal{E}_2-\mathcal{E}_2^*)^2\,d\mathfrak{r}\\
&= \int_\Omega (\mathcal{E}_1-\mathcal{E}_1^*){}_0\mathcal{D}_{\mathfrak{z}}(\mathcal{E}_1-\mathcal{E}_1^*)\,d\mathfrak{r}+\int_\Omega (\mathcal{E}_2-\mathcal{E}_2^*){}_0\mathcal{D}_{\mathfrak{z}}(\mathcal{E}_2-\mathcal{E}_2^*)\,d\mathfrak{r}\\
&= \int_\Omega (\mathcal{E}_1-\mathcal{E}_1^*)\left[\mathfrak{k}_1\Delta(\mathcal{E}_1-\mathcal{E}_1^*)-(\mathcal{E}_1-\mathcal{E}_1^*)-\left(\frac{\mathcal{E}_1\mathcal{E}_2}{1+\mathfrak{q}\mathcal{E}_1^2}-\frac{\mathcal{E}_1^*\mathcal{E}_2^*}{1+\mathfrak{q}\mathcal{E}_1^{*2}}\right)\right]d\mathfrak{r}\\
&+\int_\Omega (\mathcal{E}_2-\mathcal{E}_2^*)\left[\mathfrak{k}_2\Delta(\mathcal{E}_2-\mathcal{E}_2^*)-\left(\frac{\mathcal{E}_1\mathcal{E}_2}{1+\mathfrak{q}\mathcal{E}_1^2}-\frac{\mathcal{E}_1^*\mathcal{E}_2^*}{1+\mathfrak{q}\mathcal{E}_1^{*2}}\right)\right]d\mathfrak{r}\\
&\le \int_\Omega (\mathcal{E}_1-\mathcal{E}_1^*)(\mathfrak{k}_1\Delta(\mathcal{E}_1-\mathcal{E}_1^*)-(\mathcal{E}_1-\mathcal{E}_1^*))\,d\mathfrak{r}+\int_\Omega|\mathcal{E}_1-\mathcal{E}_1^*|\left|\frac{\mathcal{E}_1\mathcal{E}_2}{1+\mathfrak{q}\mathcal{E}_1^2}-\frac{\mathcal{E}_1^*\mathcal{E}_2^*}{1+\mathfrak{q}\mathcal{E}_1^{*2}}\right|d\mathfrak{r}\\
&+\int_\Omega (\mathcal{E}_2-\mathcal{E}_2^*)\mathfrak{k}_2\Delta(\mathcal{E}_2-\mathcal{E}_2^*)\,d\mathfrak{r}+\int_\Omega|\mathcal{E}_2-\mathcal{E}_2^*|\left|\frac{\mathcal{E}_1\mathcal{E}_2}{1+\mathfrak{q}\mathcal{E}_1^2}-\frac{\mathcal{E}_1^*\mathcal{E}_2^*}{1+\mathfrak{q}\mathcal{E}_1^{*2}}\right|d\mathfrak{r}\\
&\le \mathfrak{k}_1\int_\Omega(\mathcal{E}_1-\mathcal{E}_1^*)\Delta(\mathcal{E}_1-\mathcal{E}_1^*)\,d\mathfrak{r}-\int_\Omega(\mathcal{E}_1-\mathcal{E}_1^*)^2\,d\mathfrak{r}\\
&+\mathfrak{P}\int_\Omega|\mathcal{E}_1-\mathcal{E}_1^*|(|\mathcal{E}_1-\mathcal{E}_1^*|+|\mathcal{E}_2-\mathcal{E}_2^*|)\,d\mathfrak{r}\\
&+\mathfrak{k}_2\int_\Omega(\mathcal{E}_2-\mathcal{E}_2^*)\Delta(\mathcal{E}_2-\mathcal{E}_2^*)\,d\mathfrak{r}+\mathfrak{P}\int_\Omega|\mathcal{E}_2-\mathcal{E}_2^*|(|\mathcal{E}_1-\mathcal{E}_1^*|+|\mathcal{E}_2-\mathcal{E}_2^*|)\,d\mathfrak{r}.
\end{aligned}
\tag{19}
$$

Using Green's formula, we achieve:

$$
\begin{aligned}
{}_0\mathcal{D}_{\mathfrak{z}}\mathcal{L}_2(\mathfrak{z}) &\le -\mathfrak{k}_1\int_\Omega|\nabla(\mathcal{E}_1-\mathcal{E}_1^*)|^2\,d\mathfrak{r}-\mathfrak{k}_2\int_\Omega|\nabla(\mathcal{E}_2-\mathcal{E}_2^*)|^2\,d\mathfrak{r}-(1-\mathfrak{P})\int_\Omega(\mathcal{E}_1-\mathcal{E}_1^*)^2\,d\mathfrak{r}\\
&+\mathfrak{P}\int_\Omega(\mathcal{E}_2-\mathcal{E}_2^*)^2\,d\mathfrak{r}+2\mathfrak{P}\int_\Omega|\mathcal{E}_1-\mathcal{E}_1^*||\mathcal{E}_2-\mathcal{E}_2^*|\,d\mathfrak{r}\\
&\le -\mathfrak{k}_1\int_\Omega|\nabla(\mathcal{E}_1-\mathcal{E}_1^*)|^2\,d\mathfrak{r}-\mathfrak{k}_2\int_\Omega|\nabla(\mathcal{E}_2-\mathcal{E}_2^*)|^2\,d\mathfrak{r}-(1-\mathfrak{P})\int_\Omega(\mathcal{E}_1-\mathcal{E}_1^*)^2\,d\mathfrak{r}\\
&+\mathfrak{P}\int_\Omega(\mathcal{E}_2-\mathcal{E}_2^*)^2\,d\mathfrak{r}+\mathfrak{P}\int_\Omega\left(|\mathcal{E}_1-\mathcal{E}_1^*|^2+|\mathcal{E}_2-\mathcal{E}_2^*|^2\right)d\mathfrak{r}\\
&\le -\mathfrak{k}_1\int_\Omega|\nabla(\mathcal{E}_1-\mathcal{E}_1^*)|^2\,d\mathfrak{r}-\mathfrak{k}_2\int_\Omega|\nabla(\mathcal{E}_2-\mathcal{E}_2^*)|^2\,d\mathfrak{r}-(1-2\mathfrak{P})\int_\Omega(\mathcal{E}_1-\mathcal{E}_1^*)^2\,d\mathfrak{r}\\
&+2\mathfrak{P}\int_\Omega(\mathcal{E}_2-\mathcal{E}_2^*)^2\,d\mathfrak{r}.
\end{aligned}
\tag{20}
$$

Using Lemma 3, we obtain:

$$
\begin{aligned}
{}_0\mathcal{D}_{\mathfrak{z}}\mathcal{L}_2(\mathfrak{z}) &\le -(\mathfrak{k}_1\zeta_1-2\mathfrak{P}+1)\int_\Omega(\mathcal{E}_1-\mathcal{E}_1^*)^2\,d\mathfrak{r}-(\mathfrak{k}_2\zeta_2-2\mathfrak{P})\int_\Omega(\mathcal{E}_2-\mathcal{E}_2^*)^2\,d\mathfrak{r}\\
&\le -2\min\{\mathfrak{k}_1\zeta_1-2\mathfrak{P}+1,\mathfrak{k}_2\zeta_2-2\mathfrak{P}\}\mathcal{L}_2(\mathfrak{z}).
\end{aligned}
\tag{21}
$$

Let $\beta_{3,1}=2\min\{\mathfrak{k}_1\zeta_1-2\mathfrak{P}+1,\mathfrak{k}_2\zeta_2-2\mathfrak{P}\}$ be a strictly positive constant. Thus,

$$
\int_0^{\epsilon}\frac{1}{\beta_{3,1}}\,d\varsigma=\frac{\epsilon}{2\min\{\mathfrak{k}_1\zeta_1-2\mathfrak{P}+1,\mathfrak{k}_2\zeta_2-2\mathfrak{P}\}}<+\infty,
\tag{22}
$$

The Lyapunov function $\mathcal{L}_2$ is decreasing over the interval $0\le\mathfrak{z}<\mathfrak{z}_1^*\le\mathfrak{z}_{\max}$. This implies that $\mathcal{L}_2(\mathfrak{z})>\mathcal{L}_2(\mathfrak{z}_1^*)>\mathcal{L}_2(\mathfrak{z}_{\max})$. Furthermore, we have:

$$
\begin{aligned}
\mathcal{L}_2(\mathfrak{z}) &\le \mathcal{L}_2(0)-2\min\{\mathfrak{k}_1\zeta_1-2\mathfrak{P}+1,\mathfrak{k}_2\zeta_2-2\mathfrak{P}\}\int_0^{\mathfrak{z}}\mathcal{L}_2(s)\,d\varsigma\\
&\le \mathcal{L}_2(0)-2\min\{\mathfrak{k}_1\zeta_1-2\mathfrak{P}+1,\mathfrak{k}_2\zeta_2-2\mathfrak{P}\}\int_0^{\mathfrak{z}}\mathcal{L}_2(\mathfrak{z}_{\max})\,d\varsigma\\
&= \mathcal{L}_2(0)-2\min\{\mathfrak{k}_1\zeta_1-2\mathfrak{P}+1,\mathfrak{k}_2\zeta_2-2\mathfrak{P}\}\mathcal{L}_2(\mathfrak{z}_{\max})\mathfrak{z}.
\end{aligned}
$$

By applying Definitions 4 and 5, as $\mathfrak{z}$ approaches $\mathfrak{z}_1^*$, the function $\mathcal{L}_2(\mathfrak{z})$ tends to zero:

$$\lim_{\mathfrak{z}\to\mathfrak{z}_1^*}\mathcal{L}_2(\mathfrak{z}) \le \mathcal{L}_2(0) - 2\min\{\mathfrak{k}_1\zeta_1 - 2\mathfrak{P}+1, \mathfrak{k}_2\zeta_2 - 2\mathfrak{P}\}\mathcal{L}_2(\mathfrak{z}_{\max})\mathfrak{z}_1^* = 0. \tag{23}$$

The settling time can be defined as:

$$\mathfrak{z}_1^* = \frac{\mathcal{L}_2(0)}{2\min\{\mathfrak{k}_1\zeta_1 - 2\mathfrak{P}+1, \mathfrak{k}_2\zeta_2 - 2\mathfrak{P}\}\mathcal{L}_2(\mathfrak{z}_{\max})}.$$

Thus, $\mathcal{E}^* = \left(\mathfrak{a}-\mathfrak{b}, \mathfrak{b}\frac{1+\mathfrak{q}(\mathfrak{a}-\mathfrak{b})^2}{\mathfrak{a}-\mathfrak{b}}\right)$ represents a finite-time stable equilibrium point of the nonlinear systems (9), as stated in Theorem 1. □

5. Finite-Time Synchronization Scheme

The objective of finite-time synchronization in reaction–diffusion systems is to achieve coordinated behavior among the elements of the system within a specified and limited time duration. This ensures that the systems synchronize within a defined timeframe, which is essential for various applications such as control system design, pattern generation, and synchronization in complex networks.

In this study, we explore the response of the Degn–Harrison reaction–diffusion system, which is governed by a set of partial differential equations incorporating nonlinear reaction terms and diffusion processes. The system's behavior is described by:

$$\begin{cases} {}_0^C\mathcal{D}_{\mathfrak{z}}^{\aleph}\bar{\mathcal{E}}_1(\mathfrak{r},\mathfrak{z}) = \mathfrak{k}_1\Delta\bar{\mathcal{E}}_1 + \mathfrak{a} - \bar{\mathcal{E}}_1 - \frac{\bar{\mathcal{E}}_1\bar{\mathcal{E}}_2}{1+\mathfrak{q}\bar{\mathcal{E}}_1^2} + \mathcal{C}_1, & \mathfrak{r}\in\Omega, \mathfrak{z}>0, \\ {}_0^C\mathcal{D}_{\mathfrak{z}}^{\aleph}\bar{\mathcal{E}}_2(\mathfrak{r},\mathfrak{z}) = \mathfrak{k}_2\Delta\bar{\mathcal{E}}_2 + \mathfrak{b} - \frac{\bar{\mathcal{E}}_1\bar{\mathcal{E}}_2}{1+\mathfrak{q}\bar{\mathcal{E}}_1^2} + \mathcal{C}_2, & \mathfrak{r}\in\Omega, \mathfrak{z}>0, \\ \partial_{\bar{\mathcal{E}}_1} = \partial_{\bar{\mathcal{E}}_2} = 0, & \mathfrak{r}\in\partial\Omega, \mathfrak{z}>0, \\ \bar{\mathcal{E}}_1(\mathfrak{r},0) = \bar{\mathcal{E}}_{1,0}(\mathfrak{r}) > 0, \quad \bar{\mathcal{E}}_2(\mathfrak{r},0) = \bar{\mathcal{E}}_{2,0}(\mathfrak{r}) > 0, & \mathfrak{r}\in\Omega. \end{cases} \tag{24}$$

The synchronization discrepancies in Equations (9)–(24) are considered.

$$\mathfrak{e}(\mathfrak{r},\mathfrak{z}) = \begin{pmatrix}\mathfrak{e}_1\\ \mathfrak{e}_2\end{pmatrix} = \begin{pmatrix}\bar{\mathcal{E}}_1 - \mathcal{E}_1\\ \bar{\mathcal{E}}_2 - \mathcal{E}_2\end{pmatrix}, \tag{25}$$

In the subsequent discussion, we will determine the linear controllers $\mathcal{C}_1$ and $\mathcal{C}_2$ that drive the error system solution towards zero as $\mathfrak{z}$ approaches $\mathfrak{z}^*$.

Definition 7 ([32,33]). *If there is a specific time parameter $\mathfrak{z}^* > 0$ such that*

$$\lim_{\mathfrak{z}\to\mathfrak{z}^*}\|\mathfrak{e}_1(\mathfrak{z})\| + \|\mathfrak{e}_2(\mathfrak{z})\| = 0, \tag{26}$$

and

$$\|\mathfrak{e}_1(\mathfrak{z})\| + \|\mathfrak{e}_2(\mathfrak{z})\| \equiv 0, \quad \forall\mathfrak{z}\ge\mathfrak{z}^*, \tag{27}$$

then the derived-response systems (9)–(24) are synchronized in finite time.

Theorem 4. *The master–slave systems, denoted by Equations (9) and (24), attain stable and synchronized states within a finite duration by utilizing a two-dimensional linear control law*

$$\begin{cases}\mathcal{C}_1 = (1-2\mathfrak{P})\mathfrak{e}_1,\\ \mathcal{C}_2 = -2\mathfrak{P}\mathfrak{e}_2,\end{cases} \tag{28}$$

and the time of synchronization is estimated as

$$\mathfrak{z}_2^* = \left(\frac{\Gamma(\aleph+1)}{2\min\{\mathfrak{k}_1\zeta_1, \mathfrak{k}_2\zeta_2\}}\right)^{\aleph^{-1}}. \tag{29}$$

Proof. By integrating the control described in the theorem into the error system, we obtain the following dynamics:

$$\begin{cases} {}_0^C\mathcal{D}_\mathfrak{z}^\aleph \mathfrak{e}_1(\mathfrak{r},\mathfrak{z}) = \mathfrak{k}_1\Delta\mathfrak{e}_1 - 2\mathfrak{P}\mathfrak{e}_1 - \left(\frac{\bar{\mathcal{E}}_1\bar{\mathcal{E}}_2}{1+\mathfrak{q}\bar{\mathcal{E}}_1^2} - \frac{\mathcal{E}_1\mathcal{E}_2}{1+\mathfrak{q}\mathcal{E}_1^2}\right), & \mathfrak{r}\in\Omega,\mathfrak{z}>0,\\ {}_0^C\mathcal{D}_\mathfrak{z}^\aleph \mathfrak{e}_2(\mathfrak{r},\mathfrak{z}) = \mathfrak{k}_2\Delta\mathfrak{e}_2 - 2\mathfrak{P}\mathfrak{e}_2 - \left(\frac{\bar{\mathcal{E}}_1\bar{\mathcal{E}}_2}{1+\mathfrak{q}\bar{\mathcal{E}}_1^2} - \frac{\mathcal{E}_1\mathcal{E}_2}{1+\mathfrak{q}\mathcal{E}_1^2}\right), & \mathfrak{r}\in\Omega,\mathfrak{z}>0,\\ \partial_{\mathfrak{e}_1} = \partial_{\mathfrak{e}_2} = 0, & \mathfrak{r}\in\partial\Omega,\mathfrak{z}>0,\\ \mathfrak{e}_1(\mathfrak{r},0) = \bar{\mathcal{E}}_{1,0}(\mathfrak{r}) - \mathcal{E}_{1,0}(\mathfrak{r}), \quad \mathfrak{e}_2(\mathfrak{r},0) = \bar{\mathcal{E}}_{2,0}(\mathfrak{r}) - \mathcal{E}_{2,0}(\mathfrak{r}), & \mathfrak{r}\in\Omega. \end{cases} \tag{30}$$

We employ Lyapunov's direct method in conjunction with a positive definite Lyapunov function.

$$\mathcal{L}_3(\mathfrak{z}) = \frac{1}{2}\int_\Omega \left(\mathfrak{e}_1^2 + \mathfrak{e}_2^2\right) d\mathfrak{r}, \tag{31}$$

Using Lemmas 1–3, we have:

$$\begin{aligned} {}_0^C\mathcal{D}_\mathfrak{z}^\aleph \mathcal{L}_3(\mathfrak{z}) &= \frac{1}{2}\int_\Omega {}_0^C\mathcal{D}_\mathfrak{z}^\aleph \mathfrak{e}_1^2\, d\mathfrak{r} + \frac{1}{2}\int_\Omega {}_0^C\mathcal{D}_\mathfrak{z}^\aleph \mathfrak{e}_2^2\, d\mathfrak{r}\\ &\le \int_\Omega \mathfrak{e}_{10}\mathcal{D}_\mathfrak{z}^\aleph \mathfrak{e}_1\, d\mathfrak{r} + \int_\Omega \mathfrak{e}_{20}\mathcal{D}_\mathfrak{z}^\aleph \mathfrak{e}_2\, d\mathfrak{r}\\ &= \int_\Omega \mathfrak{e}_1\left[\mathfrak{k}_1\Delta\mathfrak{e}_1 - 2\mathfrak{P}\mathfrak{e}_1 - \left(\frac{\bar{\mathcal{E}}_1\bar{\mathcal{E}}_2}{1+\mathfrak{q}\bar{\mathcal{E}}_1^2} - \frac{\mathcal{E}_1\mathcal{E}_2}{1+\mathfrak{q}\mathcal{E}_1^2}\right)\right] d\mathfrak{r}\\ &+ \int_\Omega \mathfrak{e}_2\left[\mathfrak{k}_2\Delta\mathfrak{e}_2 - 2\mathfrak{P}\mathfrak{e}_2 - \left(\frac{\bar{\mathcal{E}}_1\bar{\mathcal{E}}_2}{1+\mathfrak{q}\bar{\mathcal{E}}_1^2} - \frac{\mathcal{E}_1\mathcal{E}_2}{1+\mathfrak{q}\mathcal{E}_1^2}\right)\right] d\mathfrak{r}\\ &\le \mathfrak{k}_1\int_\Omega \mathfrak{e}_1\Delta\mathfrak{e}_1\, d\mathfrak{r} + \mathfrak{k}_2\int_\Omega \mathfrak{e}_2\Delta\mathfrak{e}_2\, d\mathfrak{r} - 2\mathfrak{P}\int_\Omega \mathfrak{e}_1^2\, d\mathfrak{r} - 2\mathfrak{P}\int_\Omega \mathfrak{e}_2^2\, d\mathfrak{r}\\ &+ \int_\Omega (|\mathfrak{e}_1| + |\mathfrak{e}_2|)\left|\frac{\bar{\mathcal{E}}_1\bar{\mathcal{E}}_2}{1+\mathfrak{q}\bar{\mathcal{E}}_1^2} - \frac{\mathcal{E}_1\mathcal{E}_2}{1+\mathfrak{q}\mathcal{E}_1^2}\right| d\mathfrak{r}\\ &\le -\mathfrak{k}_1\int_\Omega |\nabla\mathfrak{e}_1|^2\, d\mathfrak{r} - \mathfrak{k}_2\int_\Omega |\nabla\mathfrak{e}_2|^2\, d\mathfrak{r} - 2\mathfrak{P}\int_\Omega \left(\mathfrak{e}_1^2 + \mathfrak{e}_2^2\right) d\mathfrak{r}\\ &+ \mathfrak{P}\int_\Omega (|\mathfrak{e}_1| + |\mathfrak{e}_2|)\left(|\bar{\mathcal{E}}_1 - \mathcal{E}_1| + |\bar{\mathcal{E}}_2 - \mathcal{E}_2|\right) d\mathfrak{r}\\ &\le -\mathfrak{k}_1\int_\Omega |\nabla\mathfrak{e}_1|^2\, d\mathfrak{r} - \mathfrak{k}_2\int_\Omega |\nabla\mathfrak{e}_2|^2\, d\mathfrak{r} - 2\mathfrak{P}\int_\Omega \left(\mathfrak{e}_1^2 + \mathfrak{e}_2^2\right) d\mathfrak{r} + 2\mathfrak{P}\int_\Omega \left(|\mathfrak{e}_1|^2 + |\mathfrak{e}_2|^2\right) d\mathfrak{r}\\ &\le -\mathfrak{k}_1\zeta_1\int_\Omega \mathfrak{e}_1^2\, d\mathfrak{r} - \mathfrak{k}_2\zeta_2\int_\Omega \mathfrak{e}_2^2\, d\mathfrak{r}\\ &= -2\min\{\mathfrak{k}_1\zeta_1,\mathfrak{k}_2\zeta_2\}\mathcal{L}_3(\mathfrak{z}). \end{aligned} \tag{32}$$

As the parameter $\aleph$ approaches 1 from the left, the expression ${}_0^C\mathcal{D}_\mathfrak{z}^\aleph \mathcal{L}_3(\mathfrak{z})$ converges to ${}_0\mathcal{D}_\mathfrak{z}\mathcal{L}_3(\mathfrak{z})$ [34]. This convergence implies

$${}_0\mathcal{D}_\mathfrak{z}\mathcal{L}_3(\mathfrak{z}) \le -2\min\{\mathfrak{k}_1\zeta_1,\mathfrak{k}_2\zeta_2\}\mathcal{L}_3(\mathfrak{z}), \tag{33}$$

where $\beta_{3,2} = 2\min\{\mathfrak{k}_1\zeta_1,\mathfrak{k}_2\zeta_2\}$ is a strictly positive constant. Consequently, we can derive

$$\int_0^\epsilon \frac{1}{\beta_{3,2}}\, d\zeta = \frac{\epsilon}{2\min\{\mathfrak{k}_1\zeta_1,\mathfrak{k}_2\zeta_2\}} < +\infty, \tag{34}$$

Using Theorem 1, we establish that the zero solution of the error system (30) indicates finite-time stability of the equilibrium point $(\mathfrak{e}_1,\mathfrak{e}_2) = (0,0)$. Moreover, employing Theorem 2, we infer:

$$\mathcal{L}_3(\mathfrak{z}) \leq \mathcal{L}_3(0)\mathsf{E}_{\aleph}\left(-2\min\{\mathfrak{k}_1\zeta_1, \mathfrak{k}_2\zeta_2\}\mathfrak{z}^{\aleph}\right), \quad \forall \mathfrak{z} \in [0, \mathfrak{z}_2^*), \tag{35}$$

with the settling-time

$$\mathfrak{z}_2^* = \left(\frac{\Gamma(\aleph+1)}{2\min\{\mathfrak{k}_1\zeta_1, \mathfrak{k}_2\zeta_2\}}\right)^{\aleph-1},$$

when $\mathfrak{z} \geq \mathfrak{z}_2^* = \left(\frac{\Gamma(\aleph+1)}{2\min\{\mathfrak{k}_1\zeta_1, \mathfrak{k}_2\zeta_2\}}\right)^{\aleph-1}$, we can conclude that

$$\mathcal{L}_3(\mathfrak{z}) \equiv 0, \tag{36}$$

Consequentially, the master–slave systems, denoted by Equations (9) and (24), attain stable and synchronized states within a finite duration according to Definition 7. □

6. Numerical Examples with Simulations

In this section, we present a diverse set of examples to illustrate the principles of finite-time stability and finite-time synchronization within the Degn–Harrison system. These examples explore various scenarios, including different initial conditions, parameter values, and control strategies, offering insights into the system's behavior. Through detailed analysis and numerical simulations, we aim to provide a comprehensive understanding of how finite-time stability and synchronization manifest in practical contexts, shedding light on the dynamics of the Degn–Harrison system.

The numerical simulations in these examples are conducted using the Finite Difference method, a crucial tool for analyzing fractional-order Degn–Harrison reaction–diffusion systems. This method discretizes partial differential equations into algebraic equations, enabling precise numerical approximation and detailed modeling of system dynamics. By facilitating simulations of complex phenomena, stability analysis, and parameter optimization, the Finite Difference method enhances our understanding of chemical and biological systems.

Example 1. *We define the domain* $\Omega = [0, 25]$ *and the parameter* $\mathfrak{z}$ *ranging from* $[0, 100]$. *The parameter values are selected as follows:*

Variable	Value
$\mathfrak{k}_1$	1
$\mathfrak{k}_2$	1
$\mathfrak{a}$	0.78
$\mathfrak{b}$	0.01275
$\mathfrak{q}$	0.75
$\mathfrak{P}$	0.5774
ζ_1	10^4
ζ_2	10^4
$\aleph$	0.99
$\mathbb{N}$	150

with initial conditions:

$$\begin{cases} \mathcal{E}_{1,0}(\mathfrak{r}) = 0.5(1 - \cos(5\mathfrak{r})), \\ \mathcal{E}_{2,0}(\mathfrak{r}) = 0.15(1 - \sin(4\mathfrak{r})). \end{cases} \tag{37}$$

The conditions of Theorem 3 are met:

$$|\mathcal{E}_2| < \mathfrak{K} = 0.3, \quad \mathfrak{P} \geq \max\left\{\frac{5}{4}\mathfrak{K}, \frac{1}{2\sqrt{\mathfrak{q}}}\right\} = 0.5774,$$
$$\min\{\mathfrak{k}_1\zeta_1 - 2\mathfrak{P} + 1, \mathfrak{k}_2\zeta_2 - 2\mathfrak{P}\} = 9.9988 \times 10^3. \tag{38}$$

Upon calculation, we obtain:

$$\begin{cases} \mathcal{L}_2(0) = 16.8056, \\ \mathcal{L}_2(100) = 8.4449 \times 10^{-6}, \end{cases} \tag{39}$$

The time of finite-time stability of the equilibrium point is estimated as:

$$\mathfrak{z}_1^* = \frac{\mathcal{L}_2(0)}{2\min\{\mathfrak{k}_1\zeta_1 - 2\mathfrak{P} + 1, \mathfrak{k}_2\zeta_2 - 2\mathfrak{P}\}\mathcal{L}_2(100)} = 99.5134s, \tag{40}$$

where

$$\mathcal{L}_2(99.5082) = 8.6830 \times 10^{-6}. \tag{41}$$

The figures presented in Figures 1 and 2 depict the spatiotemporal solutions of system (9) with homogeneous Neumann boundary conditions. According to Theorem 3, these solutions exemplify finite-time stability at the equilibrium point $\mathcal{E}^* = (0.7672, 0.0240)$. *To validate this assertion numerically, Figure 3 showcases the system's spatiotemporal solutions alongside the corresponding errors, focusing specifically on one-dimensional space. This visual representation compellingly illustrates that the Lyapunov function converge to zero as* $\mathfrak{z}$ *approaches* $\mathfrak{z}_1^* = 99.5134\,s$ *(as depicted in Figure 4).*

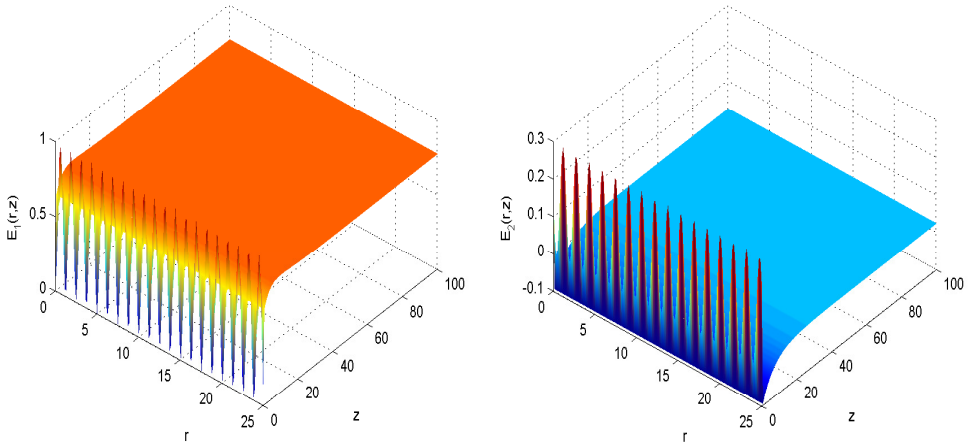

Figure 1. Dynamic behavior of the system (9): $\mathcal{E}_1(\mathfrak{r}, \mathfrak{z})$ and $\mathcal{E}_2(\mathfrak{r}, \mathfrak{z})$.

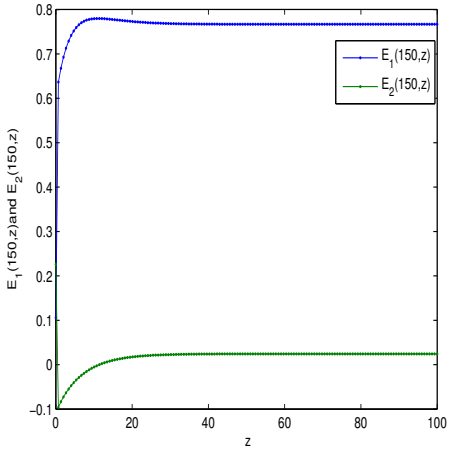

Figure 2. Solutions of the system (9): $\mathcal{E}_1(150, \mathfrak{z})$, $\mathcal{E}_2(150, \mathfrak{z})$.

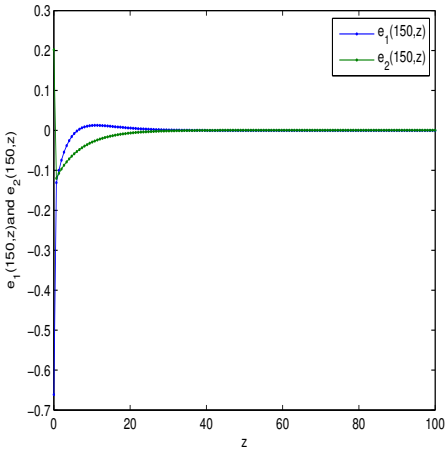

Figure 3. Solutions of the errors system (9): $\mathfrak{e}_1(150,\mathfrak{z})$, $\mathfrak{e}_2(150,\mathfrak{z})$.

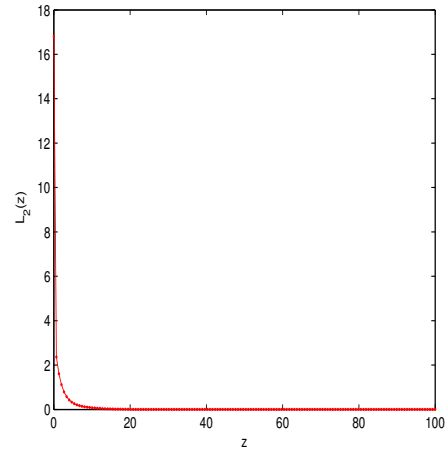

Figure 4. Estimation of the Lyapunov function $\mathcal{L}_2(\mathfrak{z})$.

Example 2. *The parameters are specified as follows:*

Parameter	Value
$\mathfrak{k}_1$	0.1885
$\mathfrak{k}_2$	0.1885
$\mathfrak{a}$	3
$\mathfrak{b}$	1.25
$\mathfrak{q}$	1
$\aleph$	0.9
$\mathfrak{P}$	3.7
ζ_1	0.6
ζ_2	0.6
$\mathbb{N}$	50

with the domain $\Omega = [0, 10]$ *and* $\mathfrak{z} \in [0, 5]$. *The initial conditions for the master–slave systems (9) and (24) are established as follows:*

$$\begin{cases} \mathcal{E}_{1,0}(\mathfrak{r}) = 1.5, \\ \mathcal{E}_{2,0}(\mathfrak{r}) = 1.5, \end{cases} \quad \begin{cases} \bar{\mathcal{E}}_{1,0}(\mathfrak{r}) = 1, \\ \bar{\mathcal{E}}_{2,0}(\mathfrak{r}) = 1, \end{cases} \tag{42}$$

We aim to formulate two controllers, denoted as $\mathcal{C}_1$ *and* $\mathcal{C}_2$, *as described below:*

$$\begin{cases} \mathcal{C}_1 = -6.4\mathfrak{e}_1, \\ \mathcal{C}_2 = -7.4\mathfrak{e}_2, \end{cases} \tag{43}$$

we have $\mathcal{L}_3(0) = 12.5$ *and*

$$\mathcal{L}_3(\mathfrak{z}) \leq M(\mathfrak{z}) = 12.5\mathrm{E}_{0.9}\left(-0.2262\mathfrak{z}^{0.9}\right), \quad \forall \mathfrak{z} \in [0, \mathfrak{z}_2^*), \tag{44}$$

The time of synchronization is estimated as:

$$\mathfrak{z}_2^* = \left(\frac{\Gamma(\aleph+1)}{2\min\{\mathfrak{k}_1\zeta_1, \mathfrak{k}_2\zeta_2\}}\right)^{\aleph-1} = 4.9937\,s, \tag{45}$$

and

$$\mathcal{L}_3(5) \approx \mathcal{L}_3(4.9937) = 4.6605 \times 10^{-6}, \tag{46}$$

where $4.9937 \leq \mathfrak{z} \leq 5$. *We can conclude that*

$$\mathcal{L}_3(\mathfrak{z}) \equiv 0. \tag{47}$$

Figures 5–7 showcase the spatiotemporal dynamics of systems (9) and (24), providing insights into both two-dimensional and one-dimensional spaces. To furnish numerical evidence, we present the spatiotemporal solutions of the error synchronization system (30) in Figures 7 and 8. This evolution clearly demonstrates that the errors converge to zero as $\mathfrak{z}$ *approaches* $\mathfrak{z}_2^* = 4.9937\,s$, *thereby illustrating the finite-time behavior of the system. Furthermore, Figure 9 exemplifies this finite-time convergence within the specified duration* $\mathfrak{z}_2^* = 4.9937\,s$.

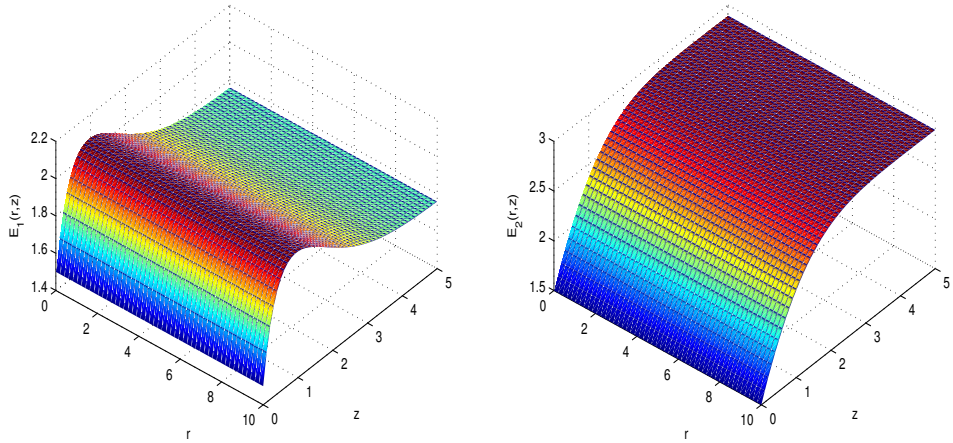

Figure 5. Dynamic behavior of the system (9): $\mathcal{E}_1(\mathfrak{r}, \mathfrak{z})$ and $\mathcal{E}_2(\mathfrak{r}, \mathfrak{z})$.

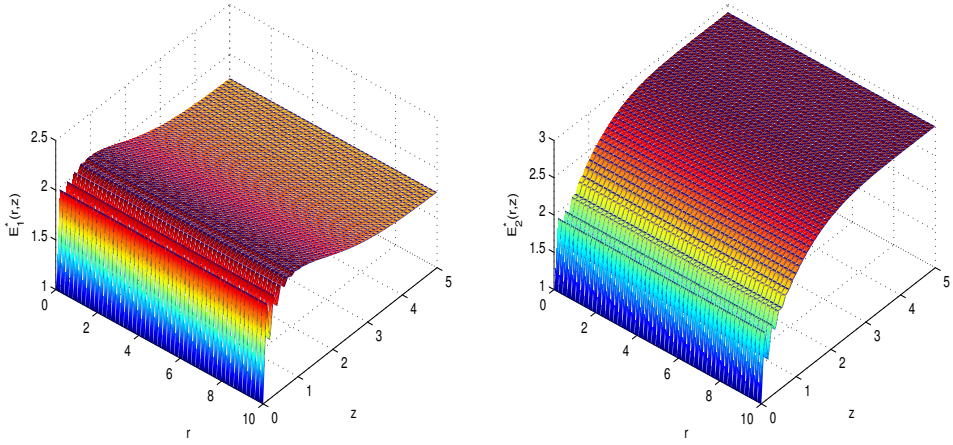

Figure 6. Dynamic behavior of the system (24): $\bar{\mathcal{E}}_1(\mathfrak{r}, \mathfrak{z})$ and $\bar{\mathcal{E}}_2(\mathfrak{r}, \mathfrak{z})$.

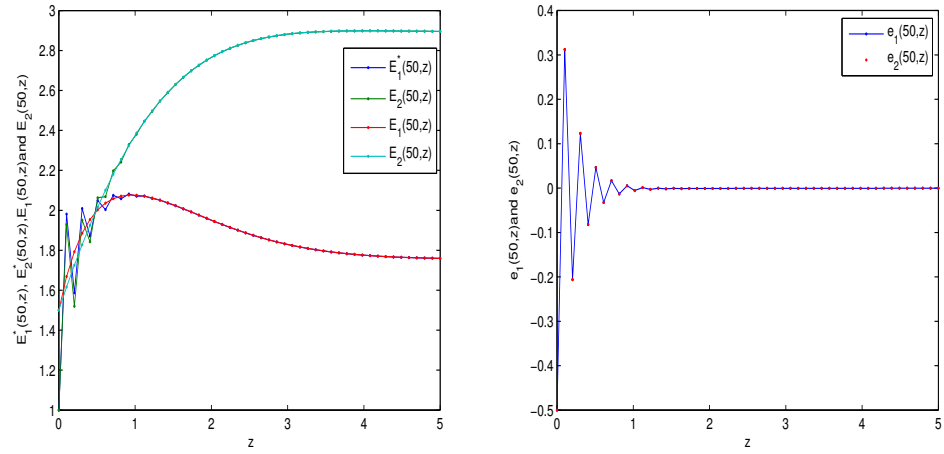

Figure 7. Solutions of the master–slave systems (9), (24), and the error system (30) at $\mathfrak{r} = 50$.

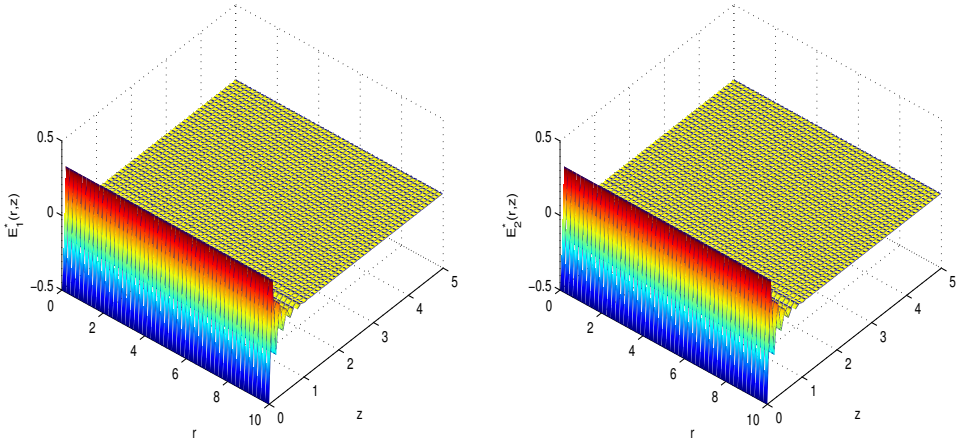

Figure 8. Dynamic behavior of the error system (30): $\mathfrak{e}_1(\mathfrak{r}, \mathfrak{z})$ and $\mathfrak{e}_2(\mathfrak{r}, \mathfrak{z})$.

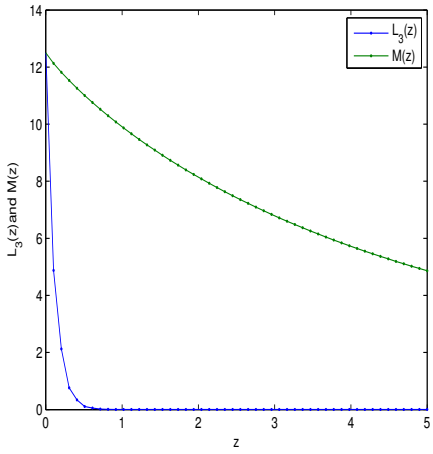

Figure 9. Estimation of the Lyapunov function $\mathcal{L}_3(\mathfrak{z})$ and $M(\mathfrak{z})$.

7. Conclusions

This study marks the beginning of an innovative exploration into the Degn–Harrison reaction–diffusion systems, introducing novel variations that promise to reveal new layers of complexity within spatiotemporal models. Our research aims to pioneer methodologies for investigating both finite-time stability and finite-time synchronization within these models, providing a comprehensive understanding of their dynamics, particularly in the context of nonlinear bacterial colonies. To initiate our investigation, we utilize the

foundational principles of Lyapunov theory to establish robust frameworks for analyzing the finite-time stability of equilibrium points and synchronization phenomena. These theoretical foundations serve as the basis for our subsequent experimental endeavors. To empirically validate the effectiveness and reliability of our proposed methodologies, we conduct extensive computational experiments. These experiments involve thorough simulations of fractional-order Degn–Harrison systems, designed to capture the dynamics and behaviors of bacterial colonies within reaction–diffusion frameworks.

As we move forward, our next phase of research will focus on extending and refining our theoretical frameworks, exploring new applications in biological systems beyond bacterial colonies, and enhancing our computational models for greater efficiency and accuracy. We plan to validate our findings through collaborative experimental work, fostering interdisciplinary collaborations to integrate diverse perspectives and expertise. Additionally, we will actively disseminate our results through various channels. Through these efforts, we aim to advance the field of reaction–diffusion systems and contribute to a deeper understanding of complex spatiotemporal phenomena. Our commitment to pushing the boundaries of knowledge in this dynamic area of research promises exciting discoveries and innovations in the near future.

Author Contributions: Conceptualization, M.A.H.; Formal analysis, I.B.; Investigation, A.A.; Methodology, W.G.A.; Resources, A.O. and A.H.; Software, S.M.; Validation, A.O.; Visualization, I.B. and M.A.H.; Writing—review and editing, A.H. All authors have read and agreed to the published version of the manuscript.

Funding: This research received no external funding.

Data Availability Statement: The original contributions presented in this study are included in the article; further inquiries can be directed to the corresponding author.

Conflicts of Interest: The authors declare no conflicts of interest.

References

1. Mesdoui, F.; Ouannas, A.; Shawagfeh, N.; Grassi, G.; Pham, V.T. Synchronization methods for the Degn-Harrison reaction-diffusion systems. *IEEE Access* **2020**, *8*, 91829–91836. [CrossRef]
2. Ouannas, A.; Abdelli, M.; Odibat, Z.; Wang, X.; Pham, V.T.; Grassi, G.; Alsaedi, A. Synchronization control in reaction-diffusion systems: Application to Lengyel-Epstein system. *Complexity* **2019**, *2019*, 2832781. [CrossRef]
3. Ambrosio, B.; Aziz-Alaoui, M.A. Synchronization and control of coupled reaction–diffusion systems of the FitzHugh–Nagumo type. *Comput. Math. Appl.* **2012**, *64*, 934–943. [CrossRef]
4. Turkyilmazoglu, M.; Alofi, A.S. Liquid Vortex Formation in a Swirling Container Considering Fractional Time Derivative of Caputo. *Fractal Fract.* **2024**, *8*, 231. [CrossRef]
5. Ouannas, A.; Wang, X.; Pham, V.T.; Grassi, G.; Huynh, V.V. Synchronization results for a class of fractional-order spatiotemporal partial differential systems based on fractional Lyapunov approach. *Bound. Value Probl.* **2019**, *2019*, 74. [CrossRef]
6. Wang, B.; Ouannas, A.; Karaca, Y.; Xia, W.F.; Jahanshahi, H.; Alkhateeb, A.F.; Nour, M. A Hybrid Approach For Synchronizing Between Two Reaction Diffusion Systems of Integer-And Fractional-Order Applied On Certain Chemical Models. *Fractals* **2022**, *30*, 2240145. [CrossRef]
7. Srivastava, M.; Ansari, S.P.; Agrawal, S.K.; Das, S.; Leung, A.Y.T. Anti-synchronization between identical and non identical fractional-order chaotic systems using active control method. *Nonlinear Dyn.* **2014**, *76*, 905–914. [CrossRef]
8. Jahanshahi, H.; Sajjadi, S.S.; Bekiros, S.; Aly, A.A. On the development of variable-order fractional hyper chaotic economic system with a nonlinear model predictive controller. *Chaos Solitons Fractals* **2021**, *144*, 110698. [CrossRef]
9. Khennaoui, A.A.; Pham, V.T.; Thoai, V.P.; Ouannas, A.; Grassi, G.; Momani, S. From Lozi map to fractional memristive Lozi map. *Eur. Phys. J. Spec. Top.* **2023**, *232*, 2385–2393. [CrossRef]
10. Khennaoui, A.A.; Ouannas, A.; Boulaaras, S.; Pham, V.T.; Taher Azar, A. A fractional map with hidden attractors: Chaos and control. *Eur. Phys. J. Spec. Top.* **2020**, *229*, 1083–1093. [CrossRef]
11. Ouannas, A.; Khennaoui, A.A.; Wang, X.; Pham, V.T.; Boulaaras, S.; Momani, S. Bifurcation and chaos in the fractional form of Hénon-Lozi type map. *Eur. Phys. J. Spec. Top.* **2020**, *229*, 2261–2273. [CrossRef]
12. Wu, Y.; Huang, T. Finite-time synchronization of chaotic systems with time-varying delays and parameter mismatches. *Nonlinear Dyn.* **2024**, *77*, 729–736.
13. Hu, J.; Wu, X. Finite-time synchronization of fractional-order chaotic systems. *Commun. Nonlinear Sci. Numer. Simul.* **2018**, *59*, 440–452.

14. Hamadneh, T.; Hioual, A.; Saadeh, R.; Abdoon, M.A.; Almutairi, D.K.; Khalid, T.A.; Ouannas, A. General methods to synchronize fractional discrete reaction–diffusion systems applied to the glycolysis model. *Fractal Fract.* **2023**, *7*, 828. [CrossRef]
15. Hamadneh, T.; Hioual, A.; Alsayyed, O.; Al-Khassawneh, Y.A.; Al-Husban, A.; Ouannas, A. The FitzHugh–Nagumo Model Described by Fractional Difference Equations: Stability and Numerical Simulation. *Axioms* **2023**, *12*, 806. [CrossRef]
16. Garvie, M.R. Finite-difference schemes for reaction–diffusion equations modeling predator–prey interactions in M ATLAB. *Bull. Math. Biol.* **2007**, *69*, 931–956. [CrossRef]
17. Houston, P.; Schwab, C.; Süli, E. Discontinuous hp-finite element methods for advection-diffusion-reaction problems. *SIAM J. Numer. Anal.* **2002**, *39*, 2133–2163. [CrossRef]
18. Bueno-Orovio, A.; Kay, D.; Burrage, K. Fourier spectral methods for fractional-in-space reaction-diffusion equations. *BIT Numer. Math.* **2014**, *54*, 937–954. [CrossRef]
19. Mesdoui, F.; Shawagfeh, N.; Ouannas, A. Global synchronization of fractional-order and integer-order N component reaction diffusion systems: Application to biochemical models. *Math. Methods Appl. Sci.* **2021**, *44*, 1003–1012. [CrossRef]
20. Song, G.; Zhang, X.; Wang, Z.; Chen, Y.; Chen, P. The asymptotic local finite-difference method of the fractional wave equation and its viscous seismic wavefield simulation. *Geophysics* **2020**, *85*, T179–T189. [CrossRef]
21. Al-Husban, A.; Djenina, N.; Saadeh, R.; Ouannas, A.; Grassi, G. A New Incommensurate Fractional-Order COVID 19: Modelling and Dynamical Analysis. *Mathematics* **2023**, *11*, 555. [CrossRef]
22. Samko, S.G.; Kilbas, A.A.; Marichev, O.I. *Fractional Integrals and Derivatives: Theory and Applications*; Gordon and Breach Science Publishers: Basel, Switzerland, 1993.
23. Feng, Z.; Xiang, Z. Finite-time stability of fractional-order nonlinear systems. *Chaos* **2024**, *34*, 023105. [CrossRef] [PubMed]
24. Ouannas, A.; Abdelmalek, S.; Bendoukha, S. *Coexistence of Some Chaos Synchronization Types in Fractional-Order Differential Equations*; Texas State University, Department of Mathematics: San Marcos, TX, USA, 2017 .
25. Aguila-Camacho, N.; Duarte-Mermoud, M.A.; Gallegos, J.A. Lyapunov functions for fractional order systems. *Commun. Nonlinear Sci. Numer. Simul.* **2014**, *19*, 2951–2957. [CrossRef]
26. Yaagoub, Z.; Danane, J.; Hammouch, Z.; Allali, K. Mathematical analysis of a fractional order two strain SEIR epidemic model. *Results Nonlinear Anal.* **2024**, *7*, 156–175.
27. Jiang, J.; Li, H.; Zhao, K.; Cao, D.; Guirao, L.G. Finite time stability and sliding mode control for uncertain variable fractional order nonlinear systems. *Adv. Differ. Equ.* **2021**, *2021*, 127. [CrossRef]
28. Fairén V.; Velarde, M.G. Time-periodic oscillations in a model for the respiratory process of a bacterial culture. *J. Math. Biol.* **1979**, *8*, 147–157. [CrossRef]
29. Lisena, B. Some global results for the Degn—Harrison system with diffusion. *Medit. J. Math.* **2017**, *14*, 91. [CrossRef]
30. Abu Falahah, I.; Hioual, A.; Omar Al-Qadri, M.; AL-Khassawneh, Y.A.; Al-Husban, A.; Hamadneh, T.; Ouannas, A. Synchronization of Fractional Partial Difference Equations via Linear Methods. *Axioms* **2023**, *12*, 728. [CrossRef]
31. Pan, J.; Liu, X.; Zhong, S. Stability criteria for impulsive reaction-diffusion Cohen-Grossberg neural networks with time-varying delays. *Math. Comput. Model.* **2010**, *51*, 1037–1050. [CrossRef]
32. Wang, L.; Yang, X.; Liu, H.; Chen, X. Synchronization in Finite Time of Fractional-Order Complex-Valued Delayed Gene Regulatory Networks. *Fractal Fract.* **2023**, *7*, 347. [CrossRef]
33. Li, Y.; Yang, X.; Shi, L. Finite-time synchronization for competitive neural networks with mixed delays and non-identical perturbations. *Neurocomputing* **2016**, *185*, 242–253. [CrossRef]
34. Podlubny, I. *Fractional Differential Equations: An Introduction to Fractional Derivatives, Fractional Differential Equations, to Methods of Their Solution and Some of Their Applications*; Elsevier: Amsterdam, The Netherlands, 1998.

Disclaimer/Publisher's Note: The statements, opinions and data contained in all publications are solely those of the individual author(s) and contributor(s) and not of MDPI and/or the editor(s). MDPI and/or the editor(s) disclaim responsibility for any injury to people or property resulting from any ideas, methods, instructions or products referred to in the content.